Quantitative analysis of cost savings and occupants' preferences in grid-interactive smart home operation

Quantitative analysis of cost savings and occupants' preferences in grid-interactive smart home operation

Many utility companies in the United States have introduced Time-of-Use (TOU) rates for homeowners with the goal of regulating electricity consumption during peak hour. The electrical appliances in homes include various thermostatically controlled devices, such as Air Conditioners (AC) for thermal comfort, and non-thermostatically controlled devices such as clothes washers. As a result, homeowners face the complicated challenge of economically operating multiple electrical appliances in their homes while maintaining comfort and convenience. This is usually due to the lack of an explicit understanding of the correlation between cost saving and the users' comfort. To understand the correlation, this paper is designed to construct a framework by integrating three major components: a multi-objective optimization method accommodating multiple competing goals with different weights, a learning-based system modelling approach describing the dynamics and thermal coupling effects of appliances, and a novel comfort index method differentiating preferred and acceptable thermal comfort. Our proposed framework can allow the indoor air temperature to fall into the "preferred" range with a marginal cost increase. The simulation result shows an additional 8 hours for the preferred thermal comfort can be achieved with only a cost increase of 1.77%.

Nomenclature

Parameters

α	Lumped parameter represents the thermal properties of the water tank.
$\overline{T_{hvac}}, \underline{T_{hvac}}$	Maximum and minimum indoor air temperatures inside the house.
$\overline{T_{wh}}, \underline{T_{wh}}$	Maximum and minimum hot water temperatures inside the water tank.
τ_1, τ_2, τ_3	Parameter for the RC model of the HVAC system represents the thermal properties of the home envelop and the indoor air.

Variables

C^k	The tariff at the time slot k.
D_{ij}	The number of time interval delay allowed for the appliance i for each energy phase j.
d_i^+, d_i^-	Deviation variable used for goal programming.
n_i	The total number of energy phase of the appliance i.

A, V	Surface area and the volume of the water tank.
a_1	Parameters associated with the solar irradiation for the RC model of the HVAC system.
m	The total number of time slots over the scheduling period.
M_1, M_2	Constant numbers used to indicate the distance between acceptable and preferred temperature.
N_{nt}	The total number of non-thermal appliances in the scheduling smart home.
P_{hvac}	The power of the HVAC system.
P_{limit}	Maximum power consumption at any given time over the scheduling period.
P_{wh}	The power of the water heater.
q	Parameter associated with the HVAC system output for the RC model.
T_{ideal}	Ideal indoor air temperature.
T_{inlet}	Inlet water temperature, the water temperature of the city cold water.
P_{ij}	The power consumption of the appliance i with energy phase j.
S_{ij}^k	System variables. Auxiliary variable
T_o^k, G^k	Weather information used for RC model. Outdoor air temperature and solar irradiation at time slot k.
t_{ij}	Operation time of the appliance i with energy phase j.
T_{ie}^k	Interior wall surface temperature at time slot k.
T_{in}^k	Indoor air temperature at time slot k.
T_{room}^k	The air temperature of the room where the water heater is located.
T_{wh}^k	Inside water temperature of the water heater at time slot k.
TP_i^k	Set of binary variables generated by user time preference intervals for the appliance i.
u_{hvac}^k	System variables. The on/off signal of the HVAC system at time slot k.
u_{wh}^k	System variables. The on/off signal of the water heater at time slot k.
$W_{cw,j}^k$	Water withdrawal from water tank due to the water usage of the energy phase j of the clothes washer.

Index

i	Index of non-thermal appliances/ index on deviation variables.	x_{ij}^{k}	System variables. The on/off signal of the appliance i with energy phase j at the time slot k.
j	Index of energy phase of the appliance i.	z_1, z_2	Variables related to the thermal comfort.
k	Index of time slots over the scheduling period.	**Intervals**	
		U_i	Time preference interval for the appliance i given by the homeowner over the scheduling period.

1 Introduction

As renewable power generation brings in more variability to grid operation, utilities have begun to offer dynamic tariffs, such as time-of-use (TOU) rate, critical peak pricing (CPP), and real-time pricing (RTP) (Sharifi, Fathi, and Vahidinasab 2017), to avoid generator use (frequency) fluctuation. To utilize such tariffs and optimize the control and coordination of flexible loads in buildings, a few grid-interactive building (GIB) operational frameworks (Katipamula et al. 2006; Marzband et al. 2018; Wang et al. 2022) have been developed, although they are still in the laboratory or field-testing phases. With the increased use of the Internet of Things (IoT) devices and smart meter technology, Home Energy Management System (Home-EMS) has become popular as one of the operational frameworks in GIB. In Home-EMS, optimal operation of appliances can be automatically assigned under dynamic tariffs. Although some Home-EMS frameworks have been shown to be effective in reducing energy costs and maintaining an acceptable level of comfort in spaces, the trade-offs between electricity costs and user's meaningful satisfaction are not well understood. For example, in (Joe 2022), (Wang et al. 2022), in order to achieve the maximum cost saving, the indoor air temperature was kept around the upper (or lower) limit of the comfort bound for a long period of time, which may not be preferred for users in practice. As a consequence, frustrated users may override their thermostats with more unnecessarily

aggressive set points, or even shut down the controls permanently, missing cost-saving opportunities. Therefore, it becomes critical to understand the correlations between cost savings and occupant trade-offs in thermal comfort and convenience.

For the analysis of comfort and cost correlations, three major components are required, including 1) a multi-objective optimization method capable of accommodating multiple competing goals, 2) an effective learning-based modelling approach capable of describing the operation dynamics of participating appliances, and 3) a meaningful comfort index which is capable of classifying user's thermal compromise. The thermal compromise here refers to the total amount of time that the indoor air temperature is not within the user's preferred temperature range, but within the acceptable range. The thermal appliances in this study are the appliances, such as the AC system and the electric water heater, whose thermal behaviour govern their outputs and run time. Non-thermal appliances have fixed power output and run time that can operate at different times of the day. The contribution of this study is an impact analysis of user's electricity cost and thermal comfort using a new comfort index and integrated framework to facilitate the optimal operation of appliances.

This study aims to develop a systematic framework that analyses the impact of user trade-off decision on electricity cost and comfort by integrating goal programming, learning-based RC network models, and a novel comfort index. Specifically, Section 2 provides the literature review. Section 3 discusses the formulations of the proposed framework. Section 4 contains detailed information and specifications about the appliances for a case study. It also illustrates data acquisition techniques. The results of the test cases are presented in Section 5, along with an analysis of the cost savings and comfort sacrifices associated with weather and user preferences. Section 6 concludes the study.

2 Literature Review

The literature review and proposed approaches of the three major components in the framework design are

introduced in this section.

2.1 Multi-objective Optimization

Multi-objective optimization (MOO) is a technique for resolving conflicts between competing objectives. Maintaining thermal comfort for a longer time means the cost of Heating, Ventilation, and Air Conditioning (HVAC) system operation will increase. Therefore, improving user thermal comfort and reducing electricity costs are two conflicting goals of Home-EMS, making it a perfect candidate for MOO. To solve MOO, we need to make a trade-off among a set of solutions rather than a single solution, because finding an optimal solution for one object may hurt the other if the objectives are conflict. A multi-objective optimization strategy should provide a set of solutions that can help users make decisions. Several works on multi-objective optimization for Home-EMS (Mostavi, Asadi, and Boussaa 2017; Izawa and Fripp 2018; Veras et al. 2018; Rocha et al. 2021; Yahia and Pradhan 2020; Chegari et al. 2021) have been conducted. Among these studies, (Mostavi, Asadi, and Boussaa 2017; Izawa and Fripp 2018; Veras et al. 2018; Rocha et al. 2021; Chegari et al. 2021) addressed the optimization problem using the multi-objective evolution algorithm (MOEA). Nevertheless, the efficiency of the MOEA needs to be improved to handle large-scale MOO problems. In (Yahia and Pradhan 2020), the authors used a deterministic optimization called compromise programming to solve the optimal scheduling problem with three objectives. However, the study did not include the thermodynamic behaviour of the HVAC system and the water heater. Although the authors considered user convenience, peak load, and electrical cost objectives, they did not involve the occupant thermal comfort. In addition, indoor air temperature can drop by 2–4 °F in 10 minutes, depending on many factors, such as the capacity of the AC and the outside weather condition. Therefore, the time interval chosen in the optimization must be short enough to accommodate the thermodynamic behaviour, creating computational challenge. Moreover, the time-delayed cycling of each non-thermal appliances can lead to more cost-saving opportunities, but make the problem more difficult to solve, details discussed in Section 3. Therefore, if both

thermodynamically controlled and non-thermodynamically controlled devices are included, the number of decision variables becomes significantly large. Goal programming demonstrates a unique benefit when dealing with many decision variables of a MOO problem with conflicting goals. That is, goal programming converts the problem into a single objective function that can be solved using linear programming techniques (Gen et al. 1989; Jones and Tamiz 2016). Additionally, goal programming allows for different weight combinations on each group of deviation functions, which corresponds to each objective in its final single objective function. Hence, by using goal programming we can study the trade-off between different weighting factors and solve the MOO problem for cost and comfort analysis in this study. This study is the first attempt of using goal programming for achieving optimal control and coordination among a complete set of typical home appliances in smart Home-EMS operation.

2.2 Thermal Model for Thermal Appliances

The second component is the scheduling of thermal appliances, which necessitates an accurate prediction of their thermodynamic behaviors. The accurate prediction will enable wise and meaningful decisions to achieve the lowest operating costs while managing thermal comfort. Numerous studies have been conducted to model the thermodynamics behaviors in buildings, ranging from sophisticated physics-based models (Wang et al. 2022; Berthou et al. 2014; Ogunsola, Song, and Wang 2014) to pure data-driven black box models (Attoue, Shahrour, and Younes 2018; Mtibaa et al. 2020; Xu et al. 2021). Among all the models, an important subset of building thermal models comprises the thermal network models derived from the standard RC (resistance-capacitance) approach, which is capable of simulating the dynamics of indoor air and interior wall surface temperatures. Among all the available RC models in the literature, they range from simplified 1R1C to complicated 6R2C used in (Berthou et al. 2014) or 5R4C models used in (Ogunsola, Song, and Wang 2014). It is likely that the more temperature nodes considered, the more accurate the model, but this may require additional computational time and sensor installation for each node measurement. A 2R2C model previously

used in (Wang et al. 2022) can sufficiently capture the thermal dynamics while remaining simple enough for parameter identification. Hence, the 2R2C model is selected to simulate the thermodynamic behaviors for the HVAC systems. Moreover, the RC network concept can be used in modelling the water heater. The 1R1C model is widely used in literature (Goh and Apt 2004; Shaad et al. 2012; Kepplinger, Huber, and Petrasch 2015) and is therefore adopted in this study. Importantly, the RC-based models can incorporate additional heat gains into the energy balance equation. This is a particularly useful feature for modelling thermal coupling effects between appliances, as heat transfer interactions are easy to establish.

2.3 Thermal Comfort index

Finally, the last major component, i.e., a comfort index method that is capable of classifying thermal compromise, is also necessary for this study. Multiple studies used upper and lower bounds on the constraint of indoor air temperature in typical single objective optimization problem (Kampelis et al. 2019; Zhang et al. 2017; Perez, Baldea, and Edgar 2016), which is an intuitive way to avoid discomfort while minimizing cost. This approach is illustrated in green dashed line (1) in Fig.1, where the x-axis represents temperature and y-axis represents the comfort reward, i.e., the summation of the comfort index that the model receives when the temperature varies. Thermal compromise cannot be evaluated in this case, and temperatures that fall within different comfort ranges are not distinguished as long as they stay within constraints. Moreover, two additional methods from the literature that address thermal comfort while minimizing energy costs are demonstrated in the figure. The brown dashed line (2) which denotes one type of thermal comfort reward strategy, is the negation of the sum of temperature differences squared, i.e., $\sum_{\mathrm{k=1}}^{\mathrm{m}} -\left(T_{hvac}^{k} - T_{ideal}\right)^2$ (Izawa and Fripp 2018). The major drawback of this method is that it penalizes for any deviation from the ideal set point in the indoor air temperature. In other words, the only preferred level of comfort is a single temperature, not a range of temperatures. As a result, this method is not desirable because the on/off operation of home HVAC systems is

not intended to maintain a constant temperature set point. Otherwise, frequent HVAC system cycling may occur, which is not desired for safe operation. The blue dashed line (3) in Fig.1 represents the thermal comfort strategy used in (Nagpal, Staino, and Basu 2020). The authors used the non-negative real-valued slack variable U to penalize over-achievement of the upper bound and under-achievement of the lower bounds of indoor temperature, respectively. Similar to the first method, this method does not penalize as long as the temperature remains within the bounds. However, the authors' purpose of using the slack variable is to avoid infeasible cases in optimal search by using penalties to allow temperature to exceed the bounds instead of terminating the optimal search as is the case in the first method.

Unlike the comfort reward method used in the literature, e.g., the methods listed in line (1)–(3) in Figure 1, our proposed comfort index provides different rewards for temperatures in the preferred range versus the acceptable range, as shown by the solid red line (4). The proposed approach allows the optimization algorithm to be tolerant of temperatures outside the preferred range when temperature exceed the user's preferred comfort level but remain within an acceptable range. The preferred temperature range for each time slot can be given by the user or derived from a meaningful comfort standard such as a Predicted Mean Vote scale (Fanger 1972) or an adaptive comfort model using machine learning algorithm (Aparicio-Ruiz et al. 2021). Sequences of two binary variables are introduced in this paper to obtain this purpose, as detailed in Section 3.

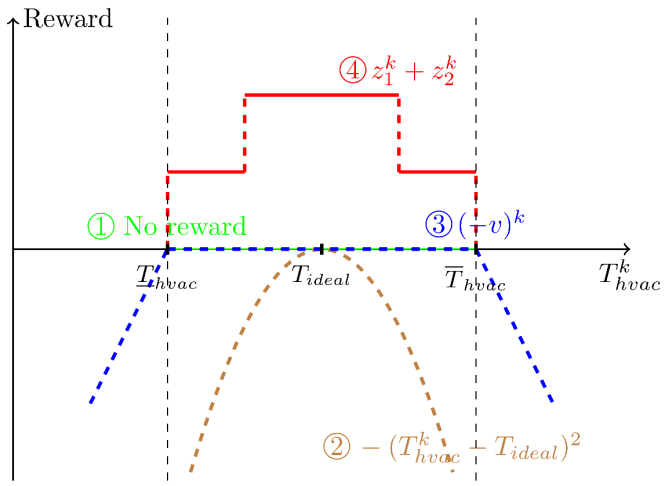

Figure 1 Schematic of comfort reward objective.

3 Methodology

This section introduces the mathematics formulation of the proposed framework used in the smart Home-EMS. We first describe the notation and decision variables used in this study in Section 3.1. We then describe each device and its associated constraints in the 3.1.1, 3.1.2, and 3.1.3 subsections below. Section 3.2 discusses two conflicting objective functions, followed by the Section 3.3, which describes a goal programming approach for solving multi-objective problems. Finally, Section 3.4 contains a summary of the mathematical formulation for the problem.

3.1 Smart Home Appliances

To model the operation of each appliance, we use a series of binary variables to represent their on/off control signals throughout the scheduling period. Before discussing each model of appliance, we introduce the notation first. Let $i \in \{I = 1,2, \dots N_{nt}\}$ denotes the number of all non-thermal appliances in a smart home, $j \in J = \{1,2, \dots n_i\}$ denote sequential energy phase of each appliance i, and $k \in K = \{1, 2, \dots m\}$ denotes each time slots of scheduling period, of which N_{nt}, n_i, and m are the number of non-thermal appliances, the energy phase

of non-thermal appliance i, and the total time slots, respectively.

3.1.1 Non-thermal Appliances

Non-thermal appliances are a group of appliances that can be turned on at any time of the day. However, once they are turned on, the output and run time depend on their energy phase, which is a subtask in the operation of a non-thermal appliance that runs for a period and consumes a specified amount of energy. For instance, washing clothes is typically divided into three phases: washing, rinsing, and extraction. Hence, the clothes washer has three energy phases. Different energy phases of the same appliance may consume a different amount of power and complete operation at a different period (a more detailed discussion of energy phases can be found in (Sou et al. 2011)).

The decision variable which represents the on/off signal for energy phase j for appliance i at each time slot k is x_{ij}^k. Besides, we use the auxiliary variables s_{ij}^k to aid the construction of constraints to regulate the on/off state of non-thermal appliances. Constraint (1) is used to regulate the operation time for each energy phase j of appliance i, where t_{ij} operation time for the energy phase, which depends on the appliance's specification (Jiang and Song 2022).

$$\sum_{k=1}^{m} x_{ij}^k = t_{ij} \quad \forall i, j, \tag{1}$$

To further regulate the operation of energy phases, the following constraints, which utilize the binary nature of x_{ij}^k and its auxiliary variable s_{ij}^k, are used.

$$x_{ij}^k + s_{ij}^k \leq 1 \quad \forall i, j, k, \tag{2}$$

$$x_{ij}^{k-1} - x_{ij}^k \leq s_{ij}^k \quad \forall i, j, k = 2, \dots, m, \tag{3}$$

$$s_{ij}^{k-1} \leq s_{ij}^k \quad \forall i, j, k = 2, \dots, m, \tag{4}$$

$$x_{ij}^{k} \le s_{ij-1}^{k} \quad \forall i, j = 2, \dots n_i, k = 1, \dots, m, \tag{5}$$

$$0 \le \sum_{k=1}^{m} \left(s_{ij-1}^{k} - \left(x_{ij}^{k} + s_{ij}^{k} \right) \right) \le D_{ij} \quad \forall i, j = 2, \dots, m, \tag{6}$$

$$x_{mj_0}^{k} \le s_{nj_{-1}}^{k} \quad \forall k. \tag{7}$$

where constraints (2) and (3) force the auxiliary variable s_{ij}^{k} to be 1 once energy phase j of appliance i turns off (i.e., x_{ij}^{k} to be 0 and x_{ij}^{k-1} to be 1). Based on constraints (2) and (3), constraint (4) ensures each energy phase of the appliance only executed once. The combination of these three constraints along with the constraint (1) ensures the energy phase j is uninterruptable. Similarly, constraint (5) ensures energy phase j turns on only after the previous energy phase turns off. Constraint (6) regulates the time delay between energy phase j and $j-1$ should be no less than time slots D_{ij}. Moreover, constraint (7)ensures that the first energy phase j_0 of appliance m turns on only after the last energy phase j_{-1} of appliance n, which aims to mimic real-life scenarios such that the clothes washer not running after the dryer. Finally, by using a series of binary sequences TP_i^k, the user time preference constraint on each appliance i is shown in (8). In this study, the user time preference, which specifies the time interval (referred as U) within which appliance i should be operated, is assumed to be provided by the user. given by:

$$\mathrm{x_{ij}^{k}} \le \mathrm{TP_{i}^{k}} \quad \forall \mathrm{i, j, k.} \tag{8}$$

3.1.2 HVAC System

For an HVAC system in the smart home, the on/off signal for each time slot u_{hvac}^{k} is a binary variable whose output depends on the home thermal dynamics. To accurately capture the home thermal dynamics, a simplified second-order thermal network model (i.e., a 2R2C model (Wang et al. 2022)) is adopted, as expressed by

$$\frac{T_{ie}^{k+1}-T_{ie}^{k}}{\Delta \mathrm{t}}=\frac{1}{\tau_1}\left(T_o^k-T_{ie}^k\right)+\frac{1}{\tau_2}\left(T_{in}^k-T_{ie}^k\right), \tag{9}$$

$$\frac{T_{in}^{k+1}-T_{in}^{k}}{\Delta \mathrm{t}}=\frac{1}{\tau_3}\left(T_{ie}^k-T_{in}^k\right)+\frac{1}{\tau_3}\left(a_1 G^k\right)+\frac{1}{\tau_3} q u_{hvac}^k, \tag{10}$$

where T_{in}, T_{ie}, and T_o represent the temperatures of the indoor air, interior wall surface, and outdoor air, respectively; G represents the solar irradiation; τ_1 represents the time constant of the virtual building envelope; τ_3 represents the time constant of the air inside the building; $\tau_2$represents the effect of the virtual envelope combined with the air; a_1 represents the effect of the solar irradiation on the building; and q represents the HVAC system's scaled cooling capacity.

The indoor air temperature is regulated by the following constraint during the scheduling period, as expressed by

$$\underline{T}_{\mathrm{hvac}} \leq T_{in}^k+\tfrac{\Delta t}{\tau_3}\left(T_{ie}^k-T_{in}^k\right)+\tfrac{\Delta t}{\tau_3}\left(a_1 G^k\right)+\tfrac{\Delta t}{\tau_3}\left(q u_{hvac}^k\right) \leq \overline{T}_{hvac} \quad \text{for } k=1,2,\ldots,m-1, \tag{11}$$

where $\underline{T}_{hvac}$ and $\overline{T}_{hvac}$ are the acceptable lower and upper temperature bounds on indoor air temperature T_{in}. Additionally, to quantify thermal comfort and account for temperature changes, the following constraints are used.

$$\underline{T}_{hvac}-T_{in}^k \leq -M_1 z_1^k \quad \forall k, \tag{12}$$

$$-\overline{T}_{hvac}+T_{in}^k \leq -M_2 z_2^k \quad \forall k, \tag{13}$$

$$z_1^k, z_2^k \in \{0,1\} \quad \forall k, \tag{14}$$

where M_1 (M_2) is a constant number that indicates the distance between the acceptable lower (upper) temperature bound and the preferred lower (upper) temperature bound; z_1^k and z_2^k are two sets of binary decision variables to distinguish between preferred and acceptable temperature ranges. To better understand how $z_1^k$and z_2^k work, the concept of *reward* $z_1^k+z_2^k$ is considered. Three examples with different rewards are shown in Figure 2, where the x-axis represents different time slot, and the y-axis is the indoor air temperature. As illustrated in

the figure, z_1^k and z_2^k will change their values based on where the indoor air temperature drops over the different temperature ranges of time slot k. If indoor air temperature is between $\underline{T}_{hvac}$ and $\underline{T}_{hvac} + M_1$, but not within the preferred range, the agent will get normal reward, i.e., $z_1^k = 0, z_2^k = 1$ in this scenario, as shown in Example 1. Similarly, if indoor air temperature is between $\overline{T}_{\text{hvac}}$ and $\overline{T}_{\text{hvac}} - M_2$, the reward is still the same, and $z_1^k = 1, z_2^k = 0$ as shown in Example 2. Once the temperature falls within the preferred range, the agent gets the highest reward, i.e., $z_1^k + z_2^k = 2$, as shown in Example 3. In this study, we assumed that both the acceptable and preferred lower and upper temperature bounds are given (i.e., $\underline{T}_{\text{hvac}}$, $\overline{T}_{hvac}$, M_1, and M_2 are given).

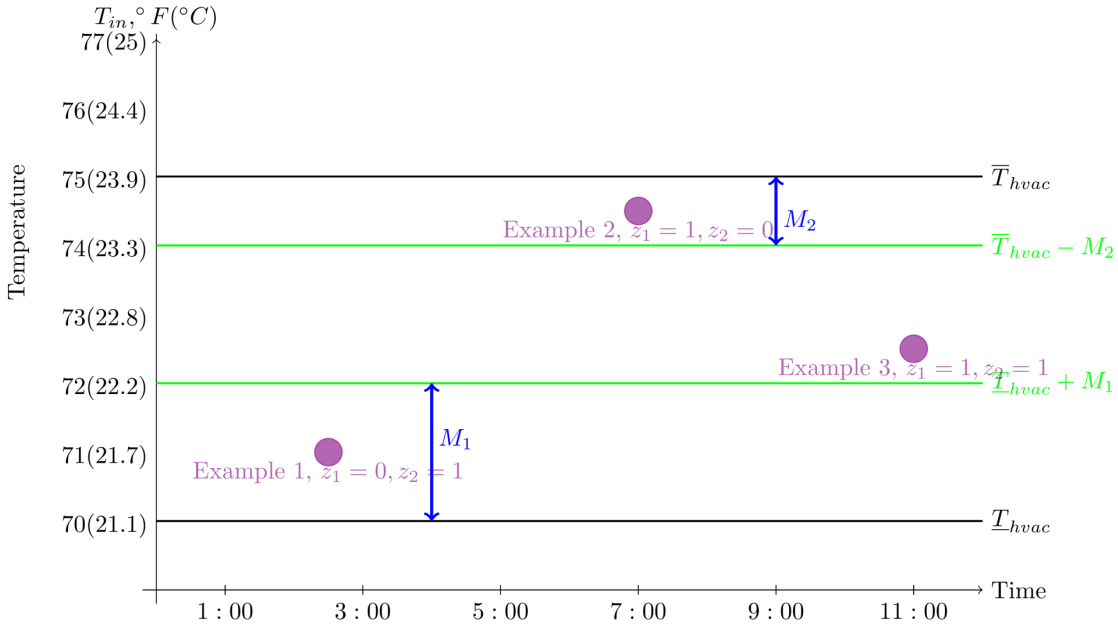

Figure 2 Comfort reward examples.

3.1.3 Electric Water Heater and the Coupling Effects

Hot water is used in many other appliances: for example, clothes washer withdraws hot water from the hot water tank. The water tank releases heat to the indoor air space, the temperature of which is determined by the HVAC

system. Therefore, accurate prediction of water heater behavior taking into account the above thermal coupling effects is important for the operation of all appliances. The RC network concept introduced in Section 2 is also widely used in the water heater modelling. In addition, the physical model can be easily modified to model the coupling effects between the water heater and other appliances. In this study, the modelling method in (Shaad et al. 2012) is adopted and modified to capture the dynamics of the hot water inside the tank. For the electric water heater, the on/off signal at each time slot u_{wh}^k is a binary decision variable whose output is depending on its thermodynamic behavior. In this study, once the clothes washer is in the washing or rinsing phase, i.e., $x_{cw\ j}^k = 1$ for j = washing or rinsing, the hot water is withdrawn from the tank, and the tank is replenished with the same amount of city cold water. Additionally, we assume the water heater is exposed to the indoor air temperature, and the changing indoor air temperature T_{in} influences the thermal leakage of the tank. The modified model is discretized as follow:

$$\frac{T_{wh}^{k+1} - T_{wh}^k}{\Delta t} = \frac{1}{\alpha}\left(\frac{A}{R}\left(T_{room}^k - T_{wh}^k\right)\right) + \frac{1}{V}\left(\sum_{cwj}^{n_{cw}} x_{cwj}^k W_{cwj}\right)\left(T_{inlet} - T_{wh}^k\right) + \frac{1}{\alpha}\left(P_{wh} u_{wh}^k\right) \quad \text{for } k = 1,2,\dots,m-1. \qquad (15)$$

where T_{wh}^k is the temperature of the water inside the tank at time slot k; α is the lumped parameter equal to $\rho C_p V$; ρ, C_p, V, A, and R are the density of water, the specific heat of water, the tank volume, surface area, and its thermal resistance, respectively; In this study, we assume that once the hot water is withdrawn, cold water with temperature T_{inlet} will enter the tank, and T_{room}^k represents the indoor air temperature at time slot k, which also equals T_{in}^k for the HVAC system. In addition, like the HVAC system, the water temperature is also regulated within a thermal comfort temperature range, $\underline{T}_{\text{wh}}$ and $\overline{T}_{wh}$ which are assumed to be given.

3.2 Cost and Comfort Objectives

There are two objectives in this study. The first is the cost of electricity, and the second is thermal comfort

mentioned in Section 3.1.2. The electricity cost is inclusive of all non-thermal appliance operating costs $\sum_{k=1}^{m} c^k\left(\sum_{i=1}^{N_{nt}}\sum_{j=1}^{n_i} x_{ij}^k P_{ij}^k\right)$, the water heater costs $\sum_{k=1}^{m} u_{wh}\, P_{wh}$, and the HVAC system costs $\sum_{k=1}^{m} u_{hvac}\, P_{hvac}$.

Besides the electricity cost, we want to maximize the total comfort index $\sum_{k=1}^{m} z_1^k + z_2^k$. As discussed in Section 3.1, the total comfort index ranges between m and $2m$ since the total number of time slots is m. For example, the optimization agent will earn m points if all temperatures exceed the preferred temperature range, or it may earn $2m$ points if all temperatures remain within the preferred temperature range. Maximizing this objective function can be interpreted as maximizing thermal comfort or maximizing the reward that the agent can obtain over the scheduling period. The proposed comfort reward method is compared to other three methods in Section 5. Moreover, cost and comfort objectives are measured and quantified in different scales. The following section discusses the goal programming technique for resolving the uneven weight problem.

3.3 Goal Programming Formulation

In goal programming, two pairs of deviation variables d_1 and d_2 are introduced. Instead of using either cost or comfort as objective function, with goal programming, the objective function becomes:

$$\min z = \sum_{i=1}^{2} w_i(d_i^+ + d_i^-), \tag{16}$$

where w_1 and w_2 are the weights correspondence with electricity cost and thermal comfort, respectively. To strike a balance between cost and comfort, we add the following constraints in the optimization problem:

$$\sum_{i=1}^{2} w_i = 1, \tag{17}$$

$$\frac{f_{\text{cost}}}{\text{target cost}} - d_1^+ + d_1^- = 1, \tag{18}$$

$$\frac{f_{\text{comfort}}}{\text{target comfort}} - d_2^+ + d_2^- = 1, \tag{19}$$

$$d_i^+ \times d_i^- = 0 \quad \forall i, \tag{20}$$

$$d_i^+, d_i^- \geq 0 \quad \forall i. \tag{21}$$

To ensure the effective control over the weights of each objective, constraint (17) regulates the sum of weights to be 1. To make sure that the distance between the objective on cost (comfort) and the target cost (target comfort) is normalized, constraint (18) (constraint (19)) is included. The target cost (target comfort) is the objective by solving the single objective optimization problem. Finally, constraint (20) and (21) indicate that $d^+(d^-)$ will be zero if the other one is non-negative. By combining (16)–(21), the weights in the objective function represent the user's intension on cost and comfort because the two objectives are normalized and sum of weights is constrained.

3.4 Summary

Based on the above discussion, we have the following formulation of the Home-EMS. The objective function is to minimize the deviation functions.

$$\min z = \sum_{i=1}^{2} w_i (d_i^+ + d_i^-), \tag{22}$$

subject to the constraints of deviation functions in goal programming

$$\sum_{i=1}^{2} w_i = 1, \tag{23}$$

$$\frac{\sum_{k=1}^{m} c^k \left(\sum_{i=1}^{N_{nt}} \sum_{j=1}^{n_i} \left(x_{ij}^k P_{ij} \right) + u_{wh}^k P_{wh} + u_{hvac}^k P_{hvac} \right)}{\text{target cost}} - d_1^+ + d_1^- = 1, \tag{24}$$

$$\frac{\sum_{k=1}^{m}(z_1^k + z_2^k)}{\text{target comfort}} - d_2^+ + d_2^- = 1, \tag{25}$$

$$d_i^+ \times d_i^- = 0 \quad \forall i, \tag{26}$$

$$d_i^+, d_i^- \geq 0 \quad \forall i, \tag{27}$$

the constraints of time operation of non-thermal appliances

$$\sum_{k=1}^{m} x_{ij}^k = t_{ij} \quad \forall i, j, \tag{28}$$

the constraints of sequential operation, uninterrupted, and non-restart properties of the energy phases,

$$x_{ij}^k + s_{ij}^k \leq 1 \quad \forall i, j, k, \tag{29}$$

$$x_{ij}^{k-1} - x_{ij}^k \leq s_{ij}^k \quad \forall i, j, k = 2, \dots, m, \tag{30}$$

$$s_{ij}^{k-1} \leq s_{ij}^k \quad \forall i, j, k = 2, \dots, m, \tag{31}$$

$$x_{ij}^k \leq s_{ij-1}^k \quad \forall i, j = 2, \dots n_i, k = 1, \dots, m, \tag{32}$$

$$x_{mj_0}^k \leq s_{nj_{-1}}^k \quad \forall k, \tag{33}$$

the constraint of time delay for the energy phases,

$$0 \leq \sum_{k=1}^{m} \left(s_{ij-1}^k - \left(x_{ij}^k + s_{ij}^k \right) \right) \leq D_{ij} \quad \forall i, j = 2, \dots, m, \tag{34}$$

the constraint of user preferences,

$$x_{ij}^k \leq TP_i^k \quad \forall i, j, k, \tag{35}$$

the constraint of the indoor air temperature controlled by the HVAC system to satisfy the user's thermal comfort,

$$\underline{T}_{hvac} \leq T_{in}^k \leq \overline{T}_{hvac} \quad \forall k, \tag{36}$$

$$\underline{T}_{hvac} - T_{in}^k \leq -M_1 z_1^k \quad \forall k, \tag{37}$$

$$-\overline{T}_{hvac} + T_{in}^k \leq -M_2 z_2^k \quad \forall k, \tag{38}$$

the constraint of the water temperature controlled by the electric water heater,

$$\underline{T}_{wh} \leq T_{wh}^{k} \leq \overline{T}_{wh} \quad \forall k, \tag{39}$$

the constraints of power usage limitation,

$$\sum_{i=1}^{N_{nt}} \sum_{j=1}^{n_i} \left(x_{ij}^{k} P_{ij}\right) + u_{wh}^{k} P_{wh} + u_{hvac}^{k} P_{hvac} \leq P_{limit} \quad \forall k, \tag{40}$$

the constraints of the decision variables of the thermal and non-thermal appliances,

$$x_{ij}^{k} \in \{0,1\} \quad \forall i, j, k, \tag{41}$$

$$s_{ij}^{k} \in \{0,1\} \quad \forall i, j, k, \tag{42}$$

$$u_{wh}^{k} \in \{0,1\} \quad \forall k, \tag{43}$$

$$u_{hvac}^{k} \in \{0,1\} \quad \forall k, \tag{44}$$

$$z_1^{k}, z_2^{k} \in \{0,1\} \quad \forall k. \tag{45}$$

4 Simulation Setup

This section provides information and specification in the simulation study. In the simulation, we want to schedule each appliance for 24-hour operation with a 10-minute time interval. Hence, if $k \in K = \{1, 2, \ldots m\}$ denotes each time slot of scheduling period, then $m = 144$. Three non-thermal appliances, namely a clothes washer, a clothes dryer, and a dishwasher, and two thermal appliances, an HVAC system and an electric hot water heater, are considered in the test problem. The water heater and the HVAC system have behaviors that are determined by the governing equations discussed in Section 3. The specifications for the water heater are adopted from (Shaad et al. 2012) and listed in Appendix along with the three non-thermal appliances. More detailed discussion of system specifications can be found in our previous published conference paper (Jiang and Song 2022), which serves as foundation of this extension work.

The HVAC system, as mentioned in (46) in Section 3, is the appliance that depends on outdoor weather conditions. The outdoor air temperature T_o and the solar irradiation G were obtained from the local weather station (Brock et al. 1995), (McPherson et al. 2007); The indoor air temperature and the interior wall surface temperature were collected in a one-story laboratory house located in Norman, Oklahoma. The house was constructed in the 1940s and had a total floor area of 1658 ft^2. The value for each parameter associated with the T_o, T_{in}, T_{ie}, G and the HVAC output q were identified by using parameter identification techniques mentioned in (Wang et al. 2022), where the model training and validation using the HVAC operational data collected in different seasons in the laboratory house were also demonstrated. In this study, for the simplified model, we chose τ_1 = 3000 as the time constant for the house envelope, τ_2 = 50 as the time constant for the indoor air, τ_3= 200, a_1 = 0.03, and $q = -2$ determined using the average value of training results tested in the same laboratory house. Note that the parameters should be retrained for applications in different houses. The HVAC system's power consumption was fixed in the model, i.e., $P_{hvac} = 2500\ W$.

Non-thermal appliances were programmed to run according to the generous user time preference in the simulation, i.e., that the dishwasher was set to start its first energy phase after 7:00 p.m., while other appliances were set to start after 10:00 a.m. All non-thermal appliances were limited to complete their final energy phase prior to 10:00 p.m. to avoid disturbing the homeowner during the late-night hours. The homeowner was allowed to give the temperature range of the thermal appliances according to their acceptance and preference. The upper bound $\overline{T}_{wh}$ and lower bound $\underline{T}_{wh}$ of the water inside the water heater were 167 °F (75 °C) and 140 °F (60 °C), respectively. The acceptable upper bound $\overline{T}_{hvac}$ and lower bound $\underline{T}_{hvac}$ of the HVAC system were 75 °F (23.9 °C) and 70 °F (21.1 °C), respectively. For the preferred temperature, the temperature range was between 72 °F (22.2 °C) and 74 °F (23.3 °C).

To perform goal programming and solve a multi-objective problem, the target cost and target comfort are required. We started with solving single objective optimization problem, which aimed to minimize electricity costs and maximize thermal comfort, respectively. These two values were used as the target cost and target comfort indices in the goal programming problem. All baseline cases were simulated using weather data on August 1st 2020, corresponding to a neutral summer day, which was neither excessively hot nor excessively cold. The TOU rate used in the test problem was 0.03 $/kWh from 0:00 a.m. to 8:10 a.m. (off-peak hour), 0.05 $/kWh from 8:20 a.m. to 1:10 p.m. (mid-peak hour), 0.18 $/kWh from 1:20 p.m. to 6:50 p.m. (on-peak hour), and 0.03 $/kWh from 7:00 p.m. to the end of the day (Jiang and Song 2022).

All results in this study were obtained by using a desktop computer equipped with an AMD 12core CPU and 32GB RAM. We used Pyomo to create the integer programming framework (Hart et al. 2012), (Hart et al. 2017) and Gurobi (Gurobi Optimization 2021) was chosen as the solver.

5 Results

In this section, the scheduling results for the three baseline cases using single-objective optimization are first discussed and compared them with the result from the goal programming. We then show detailed goal programming results for all appliances with equal weights on both objectives. Finally, we perform impact analyses and discuss the factors that affect the scheduling results.

5.1 HVAC System Results

In this subsection, we focus on the trade-off between cost and thermal comfort. The scheduling result and the HVAC system operations are compared first. Subplots (a)–(d) in Figure 3 include 24-hour scheduling results for three baseline cases using the single-objective optimization and the one for goal programming with equal weights. The light purple bars in all subplots represent the HVAC on/off signal. The red curve in Figure 3 is the

indoor air temperature and the green shaded area represents the preferred temperature range. Note that such preferred temperature range can be given by the user or derived from some comfort standards such as PMV index. Here we assume that users prefer a uniform temperature range, 72 °F (22.2 °C)–74 ° F (23.3°C) and accept a uniform temperature range 70 °F (21.1 °C)–75 °F (23.9 °C) throughout the scheduling period. The three vertical dashed lines divide the scheduling time into four segments, with "shoulder" or the mid-peak hours starting in the morning and on-peak hour starting in the afternoon. In all cases, the initial indoor air temperature, the outside weather condition, and the specifications for all appliances were kept the same and the generous user time preference is used for all non-thermal appliances.

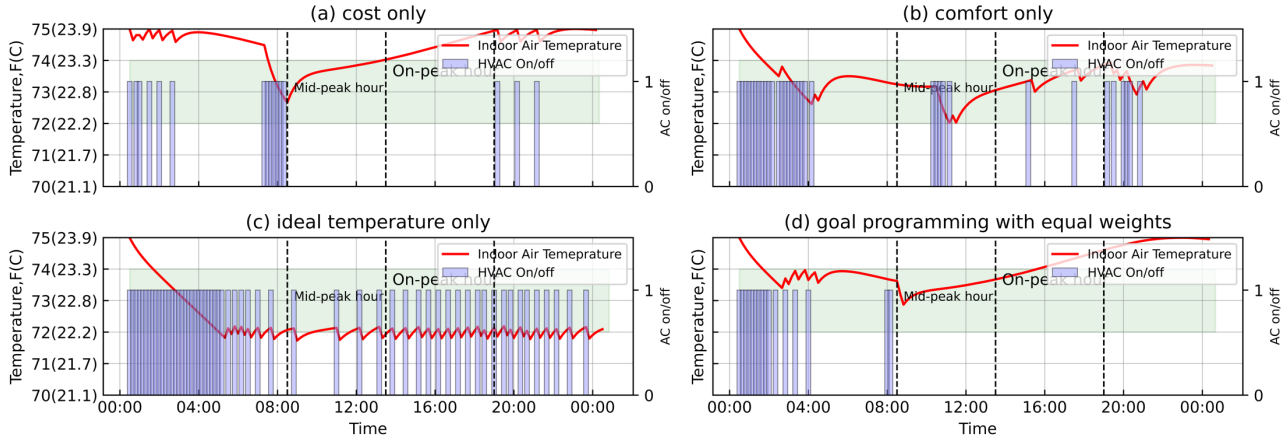

Figure 3 Home-EMS simulation results for August 1st : HVAC system on/off signal and indoor air temperature profile.

Baseline Case 1 (BS1) can be found in Figure 3(a). In this case, we solved the optimization problem with only a cost-saving objective, i.e., minimizing f_{cost} only. The total time that the indoor air temperature fell within the preferred temperature range is considered as the *comfort time*. The BS1 comfort time was 5.67 hours. The indoor temperature exceeded the preferred range at 1:00 p.m. and continuously remained within the accepted range after 1:00 p.m. The total cost of the appliances was $0.8512, which was the target cost for the

goal programming model. Appliance operation during off-peak hours accounted for 87.55% of the electricity cost, effective in avoiding operation during the mid-peak and on-peak hours.

Figure 3(b) shows Baseline Case 2 (BS2). In this case, we solved the single optimization problem with a thermal comfort objective, i.e., maximizing f_{comfort} only. In this case, the HVAC system attempted to maintain indoor air temperature inside the green shaded area. Indoor air temperature fell between 72 °F (22.2 °C)–74 °F (23.3 °C) except for the first 80 minutes of the entire 24 hours. The total electricity cost for all appliances was \$1.7028, with 45.03% from off-peak operation. The BS2 comfort time was 22.83 hours which was equivalent to 282 time slots, i.e., $\sum_{k=1}^{m} z_1^k + z_2^k = 282$. Compared with BS1, the comfort time of BS2 increased by 17.16 hours and the electricity cost increased by \$0.8516, twice that of BS1.

Another way to satisfy thermal comfort while considering temperature constraint is to incorporate the reference temperature into the objective function. The single objective in Baseline Case 3 (BS3) is to minimize $-\sum_{k=1}^{m} \left(T_{in}^k - T_{ideal}\right)^2$ only. As shown in Figure 3(c), the HVAC system made every effort to maintain temperature around 72 °F (22.2 °C). In BS3, the electricity cost was \$2.9695, which was 3.49 times the cost in BS1. Maintaining a constant temperature and ignoring the dead band of the HVAC are not preferred operations of HVAC system because the frequent on/off signals are not safe for the HVAC system.

Figure 3(d) is the optimal HVAC operation by using the proposed multi-objective optimization with equal weights on cost and comfort. Compared to BS1, the comfort time in this case was much longer, and resulted in higher electricity cost. The comfort time was shorter compared to the operation of BS2. In this case, longer HVAC operation in the morning and right before mid-peak hours made the indoor air reduced to 72.87 °F (22.7 °C), which helped avoid running the HVAC during the mid-peak and the on-peak hours.

Figure 4 summarizes the electricity costs and comfort times for all the scenarios discussed. The result of goal programming was not the most comfort strategy nor the lowest cost strategy, but a trade-off between

the two. Compared with BS1, the electricity cost was slightly increased by 1.77% ($0.0151), but comfort time was extended to 8.16 hours. Compared with BS2 in Figure 3, the electricity cost was reduced by nearly half, 49.12% ($0.8365), and the comfort time was reduced by 9 hours.

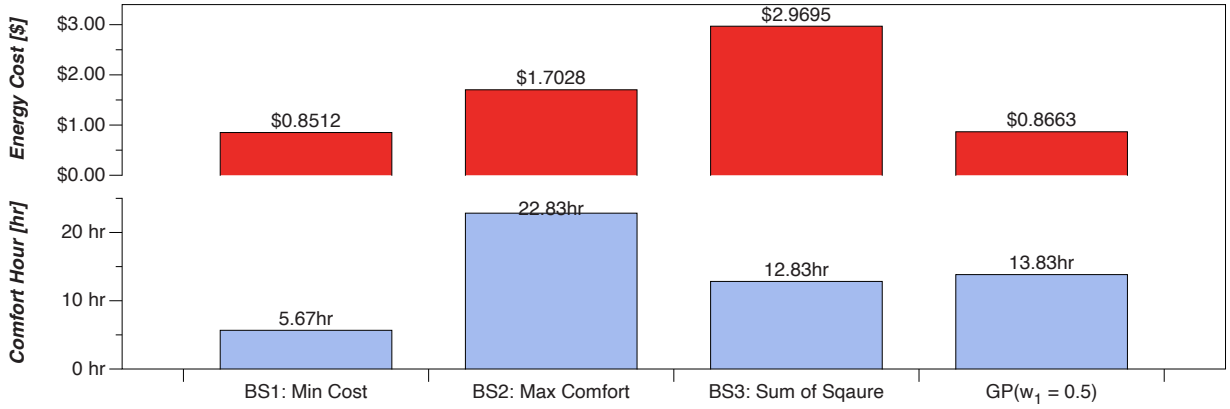

Figure 4 Cost and comfort simulation results in different scenarios for August 1st.

5.2 Detailed Operation Analysis for Goal Programming Optimization

The 24-hour scheduling results for all appliances on August 1st were obtained by using goal programming and shown in Figure 5, with equal weights assigned to cost and comfort, i.e., $w_1 = 0.5$ and $w_2 = 0.5$. Dishwasher, clothes washer, and dryer operations are listed in the top three subplots on the left. The water heater and the HVAC system operations are listed in the top two subplots on the right. The solid bars in the left three subplots represent the different energy phases for each appliance, while the solid bars in two subplots on the right represent the energy uses of water heater and HVAC. The red lines in the right two subplots represent the hot water temperature and indoor air temperature, respectively. Light blue shaded areas are the time slot associated with the mid-peak hour, and dark blue shaded areas correspond to the on-peak hour.

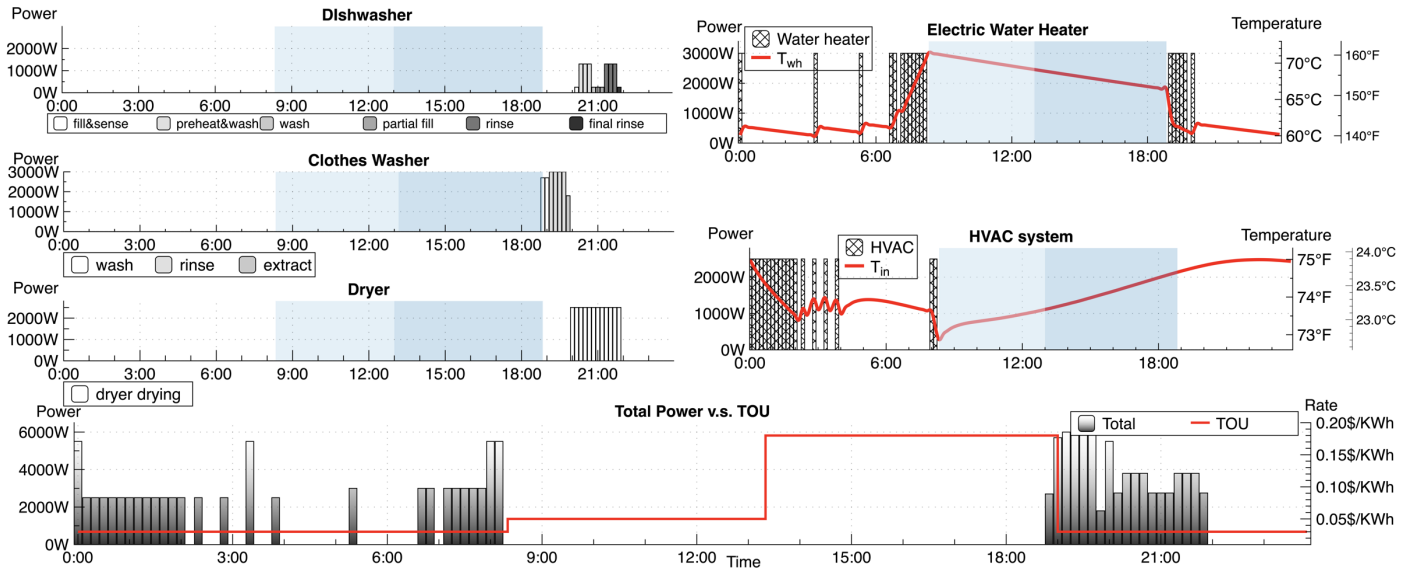

Figure 5 Detailed results for August 1st using goal programming with $w_1 = 0.5, w_2 = 0.5$

The operations of all three non-thermal appliance followed the generous user time preference, i.e. their operations were postponed until the evening to allow the other two thermal appliances to start in the morning. The water heater was connected to the clothes washer and had the pre-heating behavior—heated the water when electricity prices were low in the morning and then allowed the water temperature dropped slowly during the mid-peak and on-peak hours. When the clothes washer started in the evening, the water temperature decreased rapidly due to the hot water withdrawal but remained above the lower bound. Because the initial indoor air temperature was as high as 74.9904 °F (22.8 °C), the HVAC system ran for a longer period in the morning to bring the indoor air temperature within the preferred range and also ran right before the mid-peak hour to cool the space before price went higher. It is noted that the HVAC system scarified thermal comfort when the temperature exceeded 74 °F (23.3 °C) at 3:00 p.m. The solid bars in the last subplot stack up the total power usage of all appliances at each time slot, and the red step plot is the TOU rate. Most appliances avoided operating during on-peak hours. There was overlapping operation between appliances, and the peak load was 6000 W.

The total electricity cost was \$0.8663, of which the water heater, the HVAC system and other appliances consumed 31.17 % (\$0.2700), 27.42 % (\$0.2375), 41.41% (\$0.3588), respectively.

5.3 Impact Analysis of Weather Conditions and User Preferences

In this section, we discuss the impact of weather conditions and user preferences on the simulation results obtained when using goal programming in Home-EMS. Through the discussion, suggestions are summarized to help homeowners with decision making based on their preferences.

5.3.1 Impact of Different Weights and Weather Conditions

A series of the two goal programming results, the electricity cost and comfort time, are calculated by varying the weights in three distinct summer days: a hot summer day in July, a neutral summer day in August, and a cool day in June. To ensure that the only factor affecting the results was the weather condition, we fixed the initial indoor air temperature and interior wall surface temperature for all simulations in this subsection, i.e., T_{in}^0= 74 °F (23.3 °C) and T_{ie}^0 = 75.5 °F (23.9 °C). Because the changing interval of the weight was 0.1, there were a total of 27 results from $w_1 = 0.1$ to $w_1 = 0.9$.

Figure 6 shows details for three different weather conditions, including outdoor air temperature, solar irradiation and the wind speed. Note that the cool day started with a relatively high temperature but ended with rapid temperature drop at around noon due to the impact of a cold front.

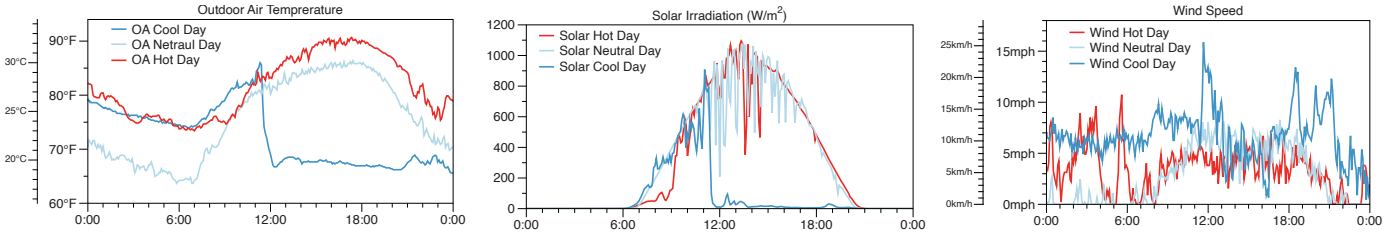

Figure 6 Weather information including outdoor air temperature, solar irradiation, and wind speed in a hot day, a neutral day and a cool day.

The solid and dashed curves in Figure 7 demonstrate the percentage increase in electricity cost savings and corresponding percentage declines in comfort time associated with the weight w_1 change, respectively, for three different weather conditions. Each weather condition had a unique switch point where the greatest cost savings improvement and comfort time loss occurred: 0.4 ($w_1 = 0.4$) for a hot day, 0.5 for a neutral day, and 0.7 for a cool day and the switch point got smaller as weather got hotter. Other weight changes only had moderate impacts on cost and comfort changes. This observation suggests that for users to achieve significant cost savings, a more aggressive weight on cost (w_1) needs to be assigned in neutral summer days than in hot summer days. For example, in our simulation results, choosing $w_1 = 0.4$ instead of $w_1 = 0.3$ could save 16.04% electricity cost on the hot summer days. However, making the same choice on the neutral summer day would only save 0.24% on cost. For temperature-sensitive users who care about thermal comfort more than the electricity cost, i.e., do not like to sacrifice preferred comfort time for too long period of time, a small weight on cost (w_1) should be assigned to hot summer days than on neutral summer days. On a hot summer day, for example, if the user chooses the weight w_1, which happens to be the switching point (for example, $w_1 = 0.4$ in this case), the comfort loss may be large compared to its adjacent smaller weight.

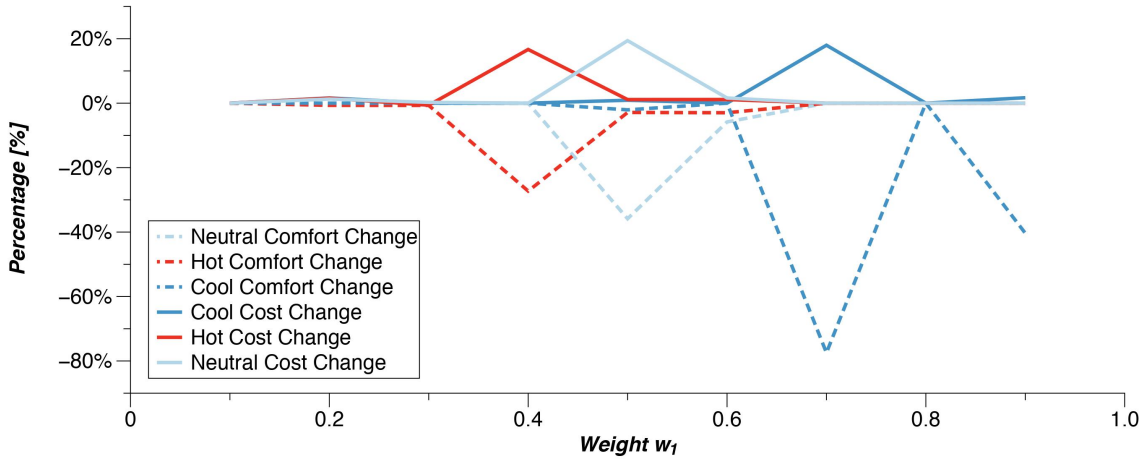

Figure 7 Percentage of cost savings increase (solid line) and percentage of comfort time decline (dashed line) with respect to weight on cost, w_1 in hot, neutral, and cold summer days.

5.3.2 Impact of User Preferences

In addition to the generous time limit, used in the previous sections, two other scenarios, namely no limit and aggressive time limit, were also created and simulated to determine the impact of user preferences on the non-thermal appliance usage. The no limit scenario refers as no limit on starting or stopping operation of non-thermal appliances, while the aggressive time limit scenario regulates all appliances must operate between 1:00 p.m. and 7:00 p.m. Each of the three scenarios was simulated using preferred temperature settings, namely 72 °F (22.2 °C)–74 °F (23.3 °C) for 24 hours. Equal weights in goal programming were also used to make the trade-off between cost and thermal comfort. For comparison, all simulation results used weather data on August 1st, 2020 (a neutral summer day).

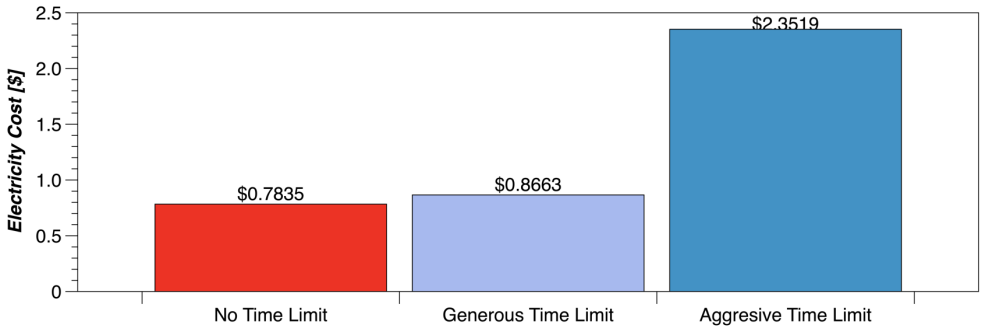

Figure 8 Total electricity cost for different user time preferences.

The simulation results are summarized in Figure 8. The bar plot in the figure demonstrates significant difference in electricity cost-saving. The cost in the aggressive time limit scenario is three times higher than the ones in the other two scenarios. The large cost difference between the aggressive time limit and the other two indicates that the time preference given by the users is one of the most significant factors affecting the cost of appliances.

The total power consumption of all appliances at TOU rate for the three user time preference scenarios are shown in Figure 9. The total power consumption for each scenario varied with the user time preferences. Because the aggressive time limit forced more non-thermal appliances to operate between 1:00 p.m. and 7:00 p.m., the appliances in this scenario consumed more energy during on-peak hours and less during off-peak hours, resulting in electricity cost that was in nearly three times higher than in the generous scenarios, as also shown in Figure 8. The no limit scenario avoided the mid-peak and on-peak hours, costing $0.2913 for non-thermal appliances. In the generous time limit scenario, all appliances completed their energy phases before 10:00 p.m., and long delays between energy phases were not allowed. Therefore, the first energy phase of the clothes washer began in the last 10 minutes of the on-peak hours, resulting in a slightly higher cost compared with no limit scenario. The operation of the clothes washer also affected the water heater, but the effect was marginal. Thus, compared to the scenario with no limit on user preferences, a generous time limit cost slightly more. It is clear that consumers' energy awareness is a critical factor in achieving energy-efficient and grid-connected homes.

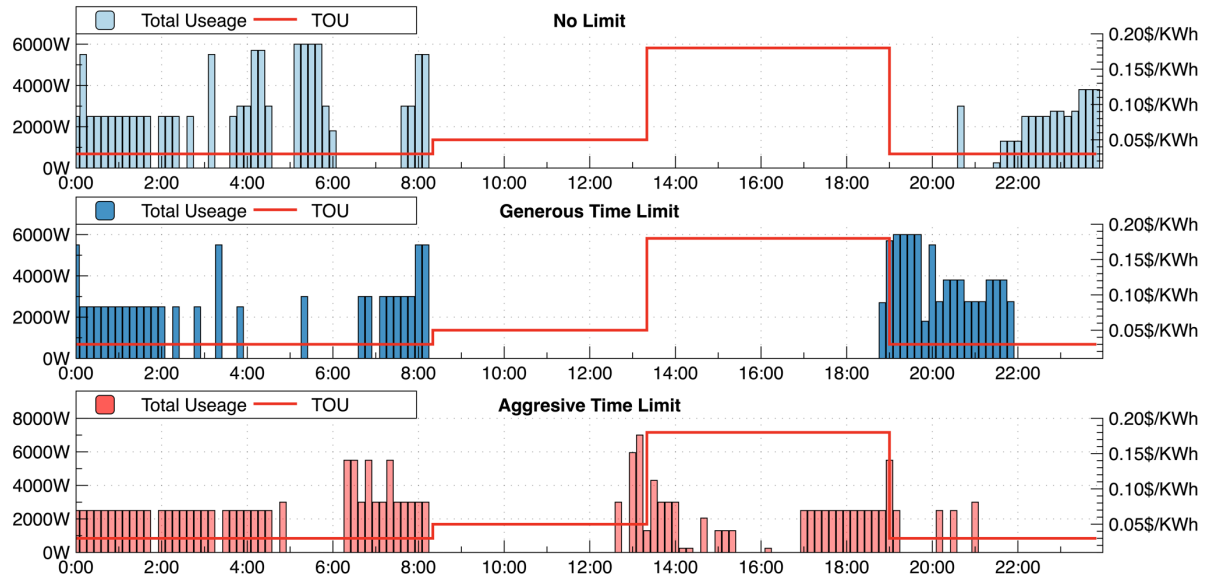

Figure 9 Total power usage under the same preferred temperature range when different user time preference $w_1 = 0.5, w_2 = 0.5$ was used in the goal programming simulation.

6 Conclusion

In this study, by using a multi-objective optimization technique, a second-order thermal model, and a novel comfort reward strategy, an optimization framework for Home-EMS is developed, simulated, and analyzed. Different from previous studies that rely on either a single temperature range or an ideal temperature setpoint, by providing the homeowner acceptable and preferred temperature ranges, the framework enables a user-defined trade-off between electricity cost and thermal comfort. The proposed framework results in an 8.16-hour extension on comfort time with only a 1.77% electricity cost increment compared with minimizing-cost only strategy, and it provides 49.12% cost reduction with a 9-hour comfort time loss compared with maximizing-comfort only strategy. We also observe that in each weather condition, there exists a unique weights combination (w_1 and w_2) which associates with the greatest cost reduction and comfort decline. This suggests a cost-sensitive user might choose more aggressive weight w_1 in colder days to achieve higher cost-saving, while a comfort-sensitive user might choose a smaller w_1 on a hotter day to avoid large comfort loss. Finally, an aggressive user time preferences on non-thermal appliances generates three times higher electricity cost than the case that user do not provide time limits.

As with simulation studies, the results reported in this study have limitations. The 2R2C model, which is used to regulate the HVAC system operation, did not consider the internal heat gain. In our case study, because the HVAC system model is built upon the data collected from an unoccupied laboratory house and because the internal heat gain generated by the appliances are relatively small, ignoring the internal heat gain is deemed acceptable. Therefore, the impact of user occupancy, which is associated with the internal heat gain, is not discussed in this study. In addition, it is assumed that the user acceptable and preferred temperature ranges

on the HVAC system and user time preference are given. Although the proposed framework can integrate with the given preference easily, deriving user thermal preference and time preference based on historical data is a focus area for next phase study.

References

Aparicio-Ruiz, Pablo, Elena Barbadilla-Martín, José Guadix, and Pablo Cortés. 2021. "KNN and Adaptive Comfort Applied in Decision Making for HVAC Systems." *Annals of Operations Research* 303 (1): 217–31. https://doi.org/10.1007/s10479-019-03489-4.

Attoue, Nivine, Isam Shahrour, and Rafic Younes. 2018. "Smart Building: Use of the Artificial Neural Network Approach for Indoor Temperature Forecasting." *Energies* 11 (2). https://doi.org/10.3390/en11020395.

Berthou, Thomas, Pascal Stabat, Raphael Salvazet, and Dominique Marchio. 2014. "Development and Validation of a Gray Box Model to Predict Thermal Behavior of Occupied Office Buildings." *Energy and Buildings* 74 (May): 91–100. https://doi.org/10.1016/j.enbuild.2014.01.038.

Brock, Fred V., Kenneth C. Crawford, Ronald L. Elliott, Gerrit W. Cuperus, Steven J. Stadler, Howard L. Johnson, and Michael D. Eilts. 1995. "The Oklahoma Mesonet: A Technical Overview." *Journal of Atmospheric and Oceanic Technology* 12 (1): 5–19. https://doi.org/10.1175/1520-0426(1995)012<0005:TOMATO>2.0.CO;2.

Chegari, B., Mohamed Tabaa, Emmanuel Simeu, Fouad Moutaouakkil, and Hicham Medromi. 2021. "Multi-Objective Optimization of Building Energy Performance and Indoor Thermal Comfort by Combining Artificial Neural Networks and Metaheuristic Algorithms." *Energy and Buildings* 239 (May): 110839. https://doi.org/10.1016/j.enbuild.2021.110839.

Fanger, Povl Ole. 1972. "Thermal Comfort, Analysis and Application in Environmental Engineering." New York: McGraw-Hill.

Gen, M., K. Ida, M. Sasaki, and J. U. Lee. 1989. "Algorithms for Solving Large-Scale 0–1 Goal Programming and Its Application to Reliability Optimization Problem." *Computers & Industrial Engineering* 17 (1): 525–30. https://doi.org/10.1016/0360-8352(89)90117-4.

Goh, Chong Hock K, and Jay Apt. 2004. "Consumer Strategies for Controlling Electric Water Heaters under Dynamic Pricing." *Carnegie Mellon Electricity Industry Center Working Paper*, February.

Gurobi Optimization, LLC. 2021. "Gurobi Optimizer Reference Manual," 969.

Hart, William E., Carl D. Laird, Jean-Paul Watson, David L. Woodruff, Gabriel A. Hackebeil, Bethany L. Nicholson, and John D. Siirola. 2017. *Pyomo — Optimization Modeling in Python*. Vol. 67. Springer Optimization and Its Applications. Cham: Springer International Publishing. https://doi.org/10.1007/978-3-319-58821-6.

Hart, William E., Carl Laird, Jean-Paul Watson, and David L. Woodruff. 2012. *Pyomo – Optimization Modeling in Python*. Springer Optimization and Its Applications. New York: Springer-Verlag. https://doi.org/10.1007/978-1-4614-3226-5.

Izawa, Andrew, and Matthias Fripp. 2018. "Multi-Objective Control of Air Conditioning Improves Cost, Comfort and System Energy Balance." *Energies* 11 (9): 2373. https://doi.org/10.3390/en11092373.

Jiang, Yilin, and Li Song. 2022. "Connected Home Energy Management for Grid-Interactive Operations: Consider Coupling Effect Among Appliances." In . Toronto, Canada: ASHRAE.

Joe, Jaewan. 2022. "Investigation on Pre-Cooling Potential of UFAD via Model-Based Predictive Control." *Energy and Buildings* 259 (March): 111898. https://doi.org/10.1016/j.enbuild.2022.111898.

Jones, Dylan, and Mehrdad Tamiz. 2016. "A Review of Goal Programming." In *Multiple Criteria Decision Analysis: State of the Art Surveys*, edited by Salvatore Greco, Matthias Ehrgott, and José Rui Figueira, 903–26. International Series in Operations Research & Management Science. New York, NY: Springer. https://doi.org/10.1007/978-1-4939-3094-4_21.

Kampelis, Nikolaos, Nikolaos Sifakis, Dionysia Kolokotsa, Konstantinos Gobakis, Konstantinos Kalaitzakis, Daniela Isidori, and Cristina Cristalli. 2019. "HVAC Optimization Genetic Algorithm for Industrial Near-Zero-Energy Building Demand Response." *Energies* 12 (11): 2177. https://doi.org/10.3390/en12112177.

Katipamula, Srinivas, David P. Chassin, Darrel D. Hatley, Robert G. Pratt, and Donald J. Hammerstrom. 2006. "Transactive Controls: A Market-Based GridWiseTM Controls for Building Systems." PNNL-15921. Pacific Northwest National Lab. (PNNL), Richland, WA (United States). https://doi.org/10.2172/901475.

Kepplinger, Peter, Gerhard Huber, and Jörg Petrasch. 2015. "Autonomous Optimal Control for Demand Side Management with Resistive Domestic Hot Water Heaters Using Linear Optimization." *Energy and Buildings*, e-nova 2013 –

Sustainable Buildings: Supply – Evaluation - Integration, 100 (August): 50–55. https://doi.org/10.1016/j.enbuild.2014.12.016.

Marzband, Mousa, Fatemeh Azarinejadian, Mehdi Savaghebi, Edris Pouresmaeil, Josep M. Guerrero, and Gordon Lightbody. 2018. “Smart Transactive Energy Framework in Grid-Connected Multiple Home Microgrids under Independent and Coalition Operations.” *Renewable Energy* 126 (October): 95–106. https://doi.org/10.1016/j.renene.2018.03.021.

McPherson, Renee A., Christopher A. Fiebrich, Kenneth C. Crawford, James R. Kilby, David L. Grimsley, Janet E. Martinez, Jeffrey B. Basara, et al. 2007. “Statewide Monitoring of the Mesoscale Environment: A Technical Update on the Oklahoma Mesonet.” *Journal of Atmospheric and Oceanic Technology* 24 (3): 301–21. https://doi.org/10.1175/JTECH1976.1.

Mostavi, Ehsan, Somayeh Asadi, and Djamel Boussaa. 2017. “Development of a New Methodology to Optimize Building Life Cycle Cost, Environmental Impacts, and Occupant Satisfaction.” *Energy* 121: 606–15. https://doi.org/10.1016/j.energy.2017.01.049.

Mtibaa, Fatma, Kim-Khoa Nguyen, Muhammad Azam, Anastasios Papachristou, Jean-Simon Venne, and Mohamed Cheriet. 2020. “LSTM-Based Indoor Air Temperature Prediction Framework for HVAC Systems in Smart Buildings.” *Neural Computing and Applications* 32 (23): 17569–85. https://doi.org/10.1007/s00521-020-04926-3.

Nagpal, Himanshu, Andrea Staino, and Biswajit Basu. 2020. “Application of Predictive Control in Scheduling of Domestic Appliances.” *Applied Sciences* 10 (February): 1627. https://doi.org/10.3390/app10051627.

Ogunsola, Oluwaseyi T., Li Song, and Gang Wang. 2014. “Development and Validation of a Time-Series Model for Real-Time Thermal Load Estimation.” *Energy and Buildings* 76 (June): 440–49. https://doi.org/10.1016/j.enbuild.2014.02.075.

Perez, Krystian X., Michael Baldea, and Thomas F. Edgar. 2016. “Integrated HVAC Management and Optimal Scheduling of Smart Appliances for Community Peak Load Reduction.” *Energy and Buildings* 123 (July): 34–40. https://doi.org/10.1016/j.enbuild.2016.04.003.

Rocha, Helder R.O., Icaro H. Honorato, Rodrigo Fiorotti, Wanderley C. Celeste, Leonardo J. Silvestre, and Jair A.L. Silva. 2021. “An Artificial Intelligence Based Scheduling Algorithm for Demand-Side Energy Management in Smart

Homes." *Applied Energy* 282 (January): 116145. https://doi.org/10.1016/j.apenergy.2020.116145.

Shaad, M., A. Momeni, C. P. Diduch, M. Kaye, and L. Chang. 2012. "Parameter Identification of Thermal Models for Domestic Electric Water Heaters in a Direct Load Control Program." In *2012 25th IEEE Canadian Conference on Electrical and Computer Engineering (CCECE)*, 1–5. Montreal, QC: IEEE. https://doi.org/10.1109/CCECE.2012.6334885.

Sharifi, Reza, S. Fathi, and Vahid Vahidinasab. 2017. "A Review on Demand-Side Tools in Electricity Market." *Renewable and Sustainable Energy Reviews* Volume 72 (January): Pages 565-572. https://doi.org/10.1016/j.rser.2017.01.020.

Sou, Kin Cheong, James Weimer, Henrik Sandberg, and Karl Henrik Johansson. 2011. "Scheduling Smart Home Appliances Using Mixed Integer Linear Programming." In *IEEE Conference on Decision and Control and European Control Conference*, 5144–49. Orlando, FL, USA: IEEE. https://doi.org/10.1109/CDC.2011.6161081.

Veras, Jaclason, Igor Silva, Plácido Pinheiro, Ricardo Rabêlo, Artur Veloso, Fábbio Borges, and Joel Rodrigues. 2018. "A Multi-Objective Demand Response Optimization Model for Scheduling Loads in a Home Energy Management System." *Sensors* 18 (10): 3207. https://doi.org/10.3390/s18103207.

Wang, Junke, Yilin Jiang, Choon Yik Tang, and Li Song. 2022. "Development and Validation of a Second-Order Thermal Network Model for Residential Buildings." *Applied Energy* 306 (January): 118124. https://doi.org/10.1016/j.apenergy.2021.118124.

Xu, Yang, Yang Xu, Weijun Gao, Weijun Gao, Fanyue Qian, and Yanxue Li. 2021. "Potential Analysis of the Attention-Based LSTM Model in Ultra-Short-Term Forecasting of Building HVAC Energy Consumption." *Frontiers in Energy Research* 9 (August). https://doi.org/10.3389/fenrg.2021.730640.

Yahia, Zakaria, and Anup Pradhan. 2020. "Multi-Objective Optimization of Household Appliance Scheduling Problem Considering Consumer Preference and Peak Load Reduction." *Sustainable Cities and Society* 55 (April): 102058. https://doi.org/10.1016/j.scs.2020.102058.

Zhang, Xuan, Wenbo Shi, Bin Yan, Ali Malkawi, and Na Li. 2017. "Decentralized and Distributed Temperature Control via HVAC Systems in Energy Efficient Buildings." *arXiv:1702.03308 [Cs]*, February. http://arxiv.org/abs/1702.03308.

Appendices

Water Heater Thermal Properties

Table 1 lists the water heater thermal properties used in our case study. Note that the thermal properties of the water heater tank (i.e., α and $\frac{\mathrm{A}}{\mathrm{R}}$) is adopted from (Shaad et al. 2012), which also includes the parameter identification and model validation based on laboratory tests.

Table 1 Water Heater Thermal Properties

Name	Value	Unit	Name	Value	Unit
ρ	997.77	$\mathrm{kg/m^3}$	T_{room}	$= T_{in}$	$^{\circ}C$
C_p	4182	$kJ/kg^{\circ}C$	T_{inlet}	15	$^{\circ}C$
$C = \rho C_p V$	$1.46 * 10^6$	$J/^{\circ}C$	T_{wh}^0	60.1	$^{\circ}C$
$G = \frac{A}{R}$	4.28	$W/^{\circ}C$	P_{wh}	30000	W

Non-thermal Appliances Specs

The three non-thermal appliances we considered in this study. Each appliance has its own energy phase, and each energy phase has a specific operation time $t_{i,j}^{\mathrm{actual}}$ and power usage. When formulating the operation constraints, the operation time equals to $\left\lceil \frac{t_{i,j}^{\mathrm{actual}}}{\text{time interval}} \right\rceil$. Note that not all energy phases of the washing machine draw hot water. Therefore, only the first two rows of the water consumption column have numbers.

Table 2 Non-thermal Appliances Specification

Type	**Phase**	**Power [W]**	**Operation [min]**	**Water [$m\text{^}3/s$]**

washer	Wash	2700	19.5	0.000035
	Rinse	3000	25.0	0.000018
	Extraction	1800	7.5	-
dishwasher	fill-sense	250	9.5	-
	preheat-wash	1300	27.5	-
	wash	250	24.5	-
	partial fill	250	8	-
	heated rinse	1300	28.5	-
	final rinse	250	10	-
dryer	drying	2500	120	-